INTERNATIONAL ATOMIC ENERGY AGENCY

INDC(CCP)-410
Distr.: G

I N D C **INTERNATIONAL NUCLEAR DATA COMMITTTEE**

New Advanced Version of Computer Code ALICE - IPPE

A. I. Dityuk, A.Yu. Konobeyev[1], V.P. Lunev, Yu. N. Shubin,

Institute of Physics and Power Engineering, 249020 Obninsk
[1] Institute of Nuclear Power Engineering, 249020 Obninsk

Abstract

A new version of the ALICE code - ALICE-IPPE - is described. The main changes are briefly outlined. The new version of ALICE-IPPE differs from the ALICE-91 in a following aspects. Algorithm for the level density calculation according to the generalized superfluid model was tested, corrected and improved. Preequilibrium cluster emission calculation was included in the code. Calculation of the alpha-particle spectra is performed with account of both the pick-up and knock-out processes. The phenomenological approach is used to describe direct channel for the deuteron emission. The triton and He-3 emission spectra are calculated according to the coalescence pick-up model of Sato, Iwamoto, Harada. Double precision calculations are used in all code. The correction taking into account gamma ray emission was made for cross-section calculations. The contribution from residual (Z,A) nucleus due to photon and following particle emission to residual (Z,A-1) or (Z-1,A-1) nucleus is considered directly. The corrections were made for the algorithm of multiple precompound proton emission spectra calculation near threshold and Kalbach systematic treatment.

1. Introduction

The knowledge of reaction cross-sections in a wide energy region is necessary to study activation and transmutation of materials irradiated in thermonuclear installations, neutron generators and accelerators-driven systems. It is also important for working out the concept on long-lived radioactive waste management [1-4]. A new version of the ALICE code - ALICE-IPPE - was developed and used for the creation Medium Energy Nuclear Data Library, MENDL-2, to study activation and transmutation of materials irradiated with nucleons of intermediate energies and for other applications. Here we outline the algorithm and the main improvements of the code as compared with previous versions.

2. Precompound nucleon emission

To obtain preequilibrium nucleon spectra the geometry dependent hybrid exciton model (GDH) has been used [5, 6]. Calculations have been performed with the formula

$$\frac{d\sigma^{pre}}{de_x} = \pi\lambda^2 \sum_{l=0}^{\infty}(2l+1)T_l \sum_{n=n_0}^{\bar{n}} R_x(n)\cdot\frac{w(p-1,h,E-Q_x-e_x)}{w(p,h,E)}\cdot\frac{l_c^x}{l_c^x + l_+^x}\cdot g\cdot D_n, \qquad (1)$$

where λ is the reduced wavelength of incident particle, T_l is the transmission coefficient calculated using optical model, e_x is the energy of nucleon emitted, Q_x is the binding energy of nucleon in compound nucleus, $w(p,h,E)$ is the density of n-exciton states having p particles and h holes ($p + h = n$) at the excitation energy E, l_c^x is the emission rate of nucleon, l_+^x is the intranuclear transition rate corresponding to absorption of nucleon in nucleus, g is the single particle level density, $R_x(n)$ is the number of x-particles in n-exciton state, D_n is the «depletion» factor for n-exciton state, n_0 is the initial exciton number.

The density of exciton states has been calculated with Strutinski-Ericson formula:

$$w(p,h,E) = \frac{g(gE-A)^{n-1}}{p!h!(n-1)!}, \qquad (2)$$

To calculate the emission rate of nucleon the following relation has been used:

$$l_c^x = \frac{(2s_x+1)m_x e_x \sigma_{inv}^x(e_x)}{\pi^2\hbar^3 g_x}, \qquad (3)$$

where s_x and m_x are spin and reduced mass for particle of x-type, σ^x_{inv} is the inverse reaction cross-section for considered particle, g_x is the single particle level density for x-particle.

The intranuclear transition rate has been calculated with the following formula:

$$l_{+}^{x} = V s_0(e_x) r_l \qquad (4)$$

where V is the velocity of nucleon moving inside the nucleus, s_0 is the Pauli principle corrected cross-section of nucleon-nucleon interaction [7], r_l is the nuclear density in the range $l\lambda < r_l < (l+1)\lambda$.

The factor $R_x(n)$ included in formula (1) was calculated for neutron induced reactions by the following way:

$$R_n(3) = (Z + 2A)/(2Z + A);$$
$$R_p(3) = 2 - R_n(3); \qquad (5)$$
$$R_x(n) = R_x(3) + (n - 3)/4.$$

The calculation of nonequilibrium spectra was carried out taking into account multiple precompound nucleon emission. According to [6] it was assumed that the number of particles emitted from a particular exciton state is equal:

$$P_{np} = P_n P_p \text{ (for emission of neutron and proton);}$$
$$P_{nn} = P_n P_n/2 \text{ (for emission of two neutrons),} \qquad (6)$$

here P_n and P_p are the total number of neutrons and protons emitted from considered n-exciton configuration.

The precompound components of spectrum for *(n,n')*, *(n,2n)* and *(n,np)* reactions were calculated with the following formulae:

$$s^{Z,A}(E_n - e) = \frac{C_n}{s_n} \cdot \frac{ds_n(e)}{de},$$

$$s^{Z,A-1}(E_n + Q_{(n,2n)} - e - \bar{e}_n) = \frac{C_{nn}/2}{s_{2n}} \cdot \frac{ds_n(e)}{de}, \qquad (7)$$

$$s^{Z-1,A-1}(E_n + Q_{(n,np)} - e - \bar{e}_{p(n)}) = \frac{C_{np}}{2}\left(\left(1 - V_p/e\right)\frac{1}{s_{np}} \cdot \frac{ds_n(e)}{de} + \frac{1}{s_{pn}}\frac{ds_p(e)}{de}\right),$$

where Z, A are characteristics of target nucleus, E_n is the energy of incident neutrons, $Q_{(n,2n)}$ and $Q_{(n,np)}$ are *(n,2n)* and *(n,np)* reaction energies, V_p is the proton Coulomb potential, C_n, C_{nn} and C_{np} - are, correspondingly, the cross-section of emission of single precompound neutrons, the cross-section of coincident emission of two precompound neutrons from the same exciton states and the cross-section of neutron and proton emission in coincidence from these states, s_n and s_{2n} are the energy integrated total preequilibrium spectra of neutrons (ds_n/de) in the energy ranges $(E - B_n)$ and $(E - B_{2n})$, corresponding to *(n,n')* and *(n,2n)* reactions, s_{np} and s_{pn} are the energy integrated total preequilibrium spectra of neutrons (ds_n/de) and protons (ds_p/de) in the energy ranges from *0* to

$E_n + Q_{(n,np)}$, $\bar{e}_n$ and $\bar{e}_p$ are the average kinetic energies of neutron and proton corresponding to the kinetic energy e of the first emitted particle.

3. Precompound clusters emission

3.1. Precompound deuteron emission

The calculations of deuteron precompound spectra were carried out in the frame of the exciton coalescence pick-up model combined with hybrid exciton model. The direct mechanism of deuteron emission was also taken into account using phenomenological approach.

The considered approach to obtain deuteron emission spectra is briefly discussed below. The calculation of deuteron differential cross-sections in the framework of the coalescence pick-up model [8,9] without taking into account the direct processes shows the considerable discrepancy between calculated and experimental data. As an example, the calculated precompound spectrum of deuterons produced by *62* MeV protons incident on ^{54}Fe is presented in Figure 1. As one can see, there is a considerable difference between calculated and experimental spectra, particularly in the high energy part. The variation of some parameters, in particular the value of imaginary part of deuteron optical potential *W* in wide limits doesn't enable to achieve the agreement. The similar conclusion can be made when the exciton model in a «closed» form is used [9].

The reason of the divergence between calculated and experimental data is connected with the calculation of deuteron emission spectra without taking into account the direct mechanism of deuteron production which gives, according to [10], the considerable contribution to differential cross-section for deuteron emission.

The contribution of the direct processes to deuteron emission can be taken into account using a phenomenological approach based on the hybrid exciton model. For this purpose let us consider the nucleon pick-up and deuteron emission from the initial configuration (*1p0h*) [11, 12]. The differential cross-section for nonequilibrium deuteron emission, formally, may be written in the following form:

$$\frac{d\sigma^{pre}}{de_d} = \sigma_{non}\left\{\frac{w^*(E - Q_d - e_d)}{w(1p,0h,E)}\cdot\frac{l_c^d}{l_c^d + l_+^d}\cdot g_d + \right.$$
$$\left. + \sum_{n=3}\sum_{l+m=2} F_{l,m}(e_d)\cdot\frac{w(p-l,h,E - Q_d - e_d)}{w(p,h,E)}\cdot\frac{l_c^d}{l_c^d + l_+^d}\cdot g_d D_n\right\}, \qquad (8)$$

where $w^*(U)$ is the density of excited states for nucleus formed after deuteron emission, g_d is the single particle level density for deuterons.

It should be noted that the second term in brackets (8) describes the part of the nonequilibrium deuteron spectrum presented in Figure 1 and calculated in paper [9].

After emission of deuteron formed by nucleon pick-up from the configuration *(p,h)* the final state of the nucleus is (*p - 1, h + 1*). Therefore the density of final state may be written as

$$w^*(U) = w(0p,1h,U) \times g g_d \qquad (9)$$

where g is a value characterizing the deuteron formation.

The comparison of the deuteron emission spectra calculated with the formula (8) and the measured spectra made it possible to establish that the g value shows the weak dependence on atomic mass number of target nucleus and may be considered as a constant with a good accuracy.

As an illustration, the results of calculations of deuteron spectra using the value obtained from the experimental data are shown in Figures 2-6 for nuclei from ^{12}C to ^{195}Au. For all nuclei the calculations have been performed using following values of parameters: $\gamma = 2 \cdot 10^{-3}$, $\sum_{l+m=2} F_{l,m} = 0.3$. The imaginary part of deuteron optical potential was assumed to be equal to $W = 16$ MeV according to Ref. [6]. The calculated deuteron spectra for neutron induced reactions at the energy *14.8* MeV are shown in Figures 2, 3.

3.2. Precompound α-emission

In the present work the spectrum of α-particles is represented as a sum of three components adequate to pick-up, knock-out and evaporation processes:

$$\frac{d\sigma}{de_a} = \frac{d\sigma^{pick-up}}{de_a} + \frac{d\sigma^{knock-out}}{de_a} + \frac{d\sigma^{evap}}{de_a} \qquad (10)$$

α -particle pick-up reaction

To describe pick-up reaction the Iwamoto-Harada model is used [20]. According to paper [2] the cross section of preequilibrium emission in the frame of hybrid model is written as:

$$\frac{d\sigma^{pick-up}}{de_a} = \sigma_{non} \sum_{n=n_0} \sum_{l+m=4} F_{lm} \frac{w(p-l,h,E-Q_a-e_a)}{w(p,h,E)} \cdot \frac{l_c^a(e_a)}{l_c^a(e_a) + l_+^a(e_a)} g_a D_n \,, \qquad (11)$$

where σ_{non} is a nonelastic interaction cross section of the incident particle with a nucleus, $w(p,h,E)$ is the density of exciton states, having p particles and h holes ($p+h=n$) at the excitation energy of composite system E, $F_{l,m}(e_a)$ is the formation probability of α-particle from l excited above the Fermy-energy and m unexcited quasiparticles in a nucleus [20], e_a is the energy of α-particle emitted from a nucleus, Q_a is the binding energy of α-particle in compound nucleus, l_c^a is the emission rate of α-particle, l_+^a is the intranuclear transition rate corresponding to α-particle absorption in a nucleus, g_a is the density of single particle states for α-particle, $D(n)$ is the depletion factor for n - exciton state, n_0 is the initial number of excitons.

Emission rate is calculated as follows:

$$l_c^a = \frac{(2s_a + 1) m_a e_a s_{inv}^a(e_a)}{p^2 \pi^3 g_a}, \qquad (12)$$

where s_a and m_a are spin and the reduced mass of a-particle , s^a_{inv} is the inverse reaction cross section.

Intranuclear transition rate due to interaction of a-particle with nucleons is equal:

$$l_+^a = 2 \cdot W_{opt}^a / \hbar \quad , \qquad (13)$$

where W_{opt}^a is the imaginary part of optical potential for a-particle. Values $F_{l,m}$ obtained in [20] were used to calculate $ds^{pick\text{-}up}/de_a$.

a-particle knock-out reactions

The modified approach [14] for a-particle knock-out process description is used in the present work. The approach developed here does not have a number of deficiencies of "prepared cluster" model [14] that have been noted in Refs. [15,22], gives the description of high energy part of nonequilibrium a-spectrum close to one of knock-out model [15] and is realized more simply in numerical calculations as compared with [15].

Three-component system is considered which consists of neutrons, protons and a-particles. The state density of such system can be described by modified Strutinsky-Ericson formula:

$$w(p, \tilde{p}, n, \tilde{n}, a, \tilde{a}) = \frac{g_p^{p+\tilde{p}} g_n^{n+\tilde{n}} g_a^{a+\tilde{a}}}{p!n!a!\tilde{p}!\tilde{n}!\tilde{a}!} \cdot \frac{E^{n-1}}{(n-1)!}, \qquad (14)$$

where $p, \tilde{p}, n, \tilde{n}, a, \tilde{a}$ are numbers of protons, neutrons, a-particles and corresponding holes in n-exciton state ($n = p + \tilde{p} + n + \tilde{n} + a + \tilde{a}$); g_p,, g_n,, g_α are single-particle state densities for protons, neutrons, and a-particles.

The ratio of state density for the system after α-emission and for compound nucleus that defines the α-emission spectrum can be expressed through the ratio of densities for one-component system. The equation to calculate α-particle spectrum can be written in this case as follows:

$$\frac{ds^{knock-out}}{de_a} = s_{non} \sum_{n=n_0} j_a \cdot \frac{g}{g_a p} \cdot \frac{w(p-1, h, E - Q_a - e_a)}{w(p, h, E)} g_a \frac{l_c^a(e_a)}{l_c^a(e_a) + l_+^a(e_a)} \cdot D_n, \qquad (15)$$

where j_a is the probability of interaction of incident particle with the "prepared" α-cluster [22].

Nonequilibrium emission of a-particles at the energies higher than 100 MeV

The emission of nonequilibrium α-particles after nonequilibrium emission of neutron or proton have to be taken into account at energies higher than 100 MeV. In this case the formula for the preequilibrium emission spectra of α-particle formed due to pick-up process and emitted after preequilibrium nucleon, can be written as follows:

$$\frac{d\sigma_2^{pick-up}}{de_a} = \sigma_{non} \sum_{x=p,n}^{2} \sum_{n=n_0} R_x(n) \cdot \frac{w(p-1,h,E-Q_x-e_x)}{w(p,h,E)} \cdot \frac{l_c^x(e_x)}{l_c^x(e_x)+l_+^x(e_x)} g_x D_n$$
$$\times \sum_{n'=p+h-1} \sum_{l+m=4} F_{l,m}(e_a) \frac{w(p'-l,h',E-Q_x-e_x-Q_a-e_a)}{w(p',h',E-Q_x-e_x)} \frac{l_c^a(e_a)}{l_c^a(e_a)+l_+^a(e_a)} g_a D_{n'} , \quad (16)$$

where x is a neutron/proton index, Q_x is the binding energy of particle x in a compound nucleus, $R_x(n)$ is the factor describing the number of protons and neutrons in n-exciton state, Q_a is the separation energy of α-particle in the nucleus after emission of particle x.

The analogous formula can be written for the component corresponding to α-particle knock-out process that occurs after preequilibrium nucleon emission. It involves a preformation factor φ_α.

$$\frac{d\sigma_2^{knock-out}}{de_a} = \sigma_{non} \sum_{x=p,n}^{2} \sum_{n=n_0} R_x(n) \cdot \frac{w(p-1,h,E-Q_x-e_x)}{w(p,h,E)} \cdot \frac{l_c^x(e_x)}{l_c^x(e_x)+l_+^x(e_x)} g_x D_n$$
$$\times \sum_{n'=p+h-1} j_a \frac{g}{g_a p'} \frac{w(p'-1,h',E-Q_x-e_x-Q_a-e_a)}{w(p',h',E-Q_x-e_x)} \frac{l_c^a(e_a)}{l_c^a(e_a)+l_+^a(e_a)} g_a D_{n'} , \quad (17)$$

Parameters of the model

Parameters of the model are the sum of the probability of α-particle formation $SF_{l,m}$ and interaction probability of incident nucleons with the "prepared" α-particle j_a. Moreover the uncertainty in the single particle state density g_a and the imaginary part of the optical potential W^a_{opt} for α-particle exists. The values of $SF_{l,m}$ and j_a in formulas (11) and (15) can be determined independently. At *90* MeV incident energy the knock-out model describes the high energy part of experimental α-spectra [19] where component $d\sigma^{pick-up}/de_a$ gives a small contribution. At the same time the soft part of nonequilibrium spectrum is determined by pick-up mechanism (see Ref. [21]). For this reason $SF_{l,m}$ and φ_α can be obtained from the comparison between calculated and experimental spectra if the values of g_a and the imaginary part of the optical potential W^a_{opt} are known.

There exist various theoretical estimations of g_a: $g_a = g/4.0$ [14], $g_a = g/8.0$ [22], $g_a = A/10.36$ [23], $g_a = 4g$ [24], where g is the single particle state density for nucleon. The uncertainty in g_a, however has not much importance for the calculation of α-spectra, as far as the variation of g_a leads to redefining of other parameters, for example W^a_{opt}. In the present work g_a is chosen to be g.

The energy dependence of W^a_{opt} was determined from the comparison of theoretical and experimental α-particle spectra for proton induced reactions at energies of 18 - 90 MeV, [16,19,25-28]. The cross sections of *(n,a)* reactions obtained from the analysis of various experiments at *14.5* MeV [29] for 42 nuclei having nuclear numbers $Z > 60$ were used also.

The following values of parameters were used in the calculations of this work: $SF_{l,m} = 0.3$, and $j_a = 0.012$. The single particle state density for α-particles was $g_a = A/13$. The imaginary part of optical potential was calculated as follows: $W^a_{opt} = e_a \times W'/e_0$ at $e_a < e_0$ and $W^a_{opt} = W'$ at $e_a > e_0$, where e_a is α-particle energy, $W' = bW_0$, W_0 - is the value of the imaginary part of optical potential in a center of a nucleus, $e_0 = 0.228A$ and $b = 0.25$. The value of W_0 was taken from Refs. [30, 31]:

$$W_0 = 10. + 0.345(A-2Z) \text{ MeV}. \quad (16)$$

On the base of the developed approach the calculations of spectra and excitation functions for nucleon induced α-particle emission were performed in a wide range of nuclei. Some results are shown in Figures 7-14. The calculated and experimental [25-27] α-particle spectra for tin isotopes irradiated by protons with the energy of *18-62* MeV are shown in Figures 7,8. The measured [27,32] and calculated α-spectra for iron isotopes irradiated by *14.8* MeV neutrons and *39* MeV and *62* MeV protons are shown in Figures 9,10. Together with calculated total spectra the contributions of the components corresponding to pick-up and knock-out mechanisms and evaporation spectra are shown in Figures 7-12 also. From the comparison of calculated and experimental data shown in Figures 7-12 one can see that at relatively low incident energies the nonequilibrium α-particle emission is due to the pick-up mechanism. The contribution of knock-out processes increases as the incident particle energy increases. Thus the knock-out mechanism determines the high energy part of the α-spectrum.

This conclusion about the role of various mechanisms of α-particle emission is in accordance with the results of Refs. [12,13,17,18]. In Refs. [13,17,18], the experimental spectra of α-particles for the reactions induced by *12-20* MeV energy neutrons were analyzed on the base of DWBA method. It was shown that at these energies the pick-up process dominates in nonequilibrium α-particle emission. In Kalbach paper [12], the parametrization of the pick-up and knock-out contributions has been performed using phenomenological relations and experimental data for reactions at energies up to *62* MeV. According to Kalbach [12], the α-particle emission occurs

predominantly as pick-up process, the knock-out process contribution is observable in the high energy part of the *a*-spectrum only.

The experimental [19] and calculated α-spectra for the reactions induced by *90* MeV protons on ^{27}Al, ^{58}Ni and ^{209}Bi are compared in Figures 11,12. The calculations were performed taking into account the preequilibrium α-emission following after the emission of preequilibrium neutron or proton. One can see that the agreement of the calculation results and experimental data is achieved by the account of all various mechanisms of α-particle formation. The significance of multiple preequilibrium emission is shown in Figure 13. The calculated contributions of the first preequilibrium α-particle and α-particles emitted after preequilibrium neutron and proton to the total spectrum are shown for the $^{209}Bi(p,a)x$ reaction. One can see that the sum of the first preequilibrium α-particle only and the evaporation emission gives a poor description of the experimental data. Similar conclusion arises from the comparison of the calculations and the measurements of other characteristics of the nuclear reactions. The cross sections for nonequilibrium α-particle emission for the reactions on ^{202}Hg, obtained from the analysis of experimental data [33] and calculated in the present work, are shown in Figure 14. The calculated results for the first preequilibrium α-particle, the total cross section for α-particle emission, and the pick-up contribution to this cross section are given in the Figure 14. It is seen that a satisfactory description of experimental data is obtained only after taking into account the multiple α-particle emission and the pick-up and knock-out mechanism contributions.

4. Nuclear level density

The nuclear level density was calculated using the phenomenological approach [34] based on the generalised superfluid model for all nuclei formed in evaporation cascade.

The level density in generalised superfluid model can be described if we subdivide the excited states into quasiparticle, coherent and colective ones. Then nuclear level density is presented as

$$r(U) = r_{qp}(U') K_{vib}(U') K_{rot}(U'), \qquad (18)$$

where $r_{qp}(U')$ - is the density of quasiparticle (non-collective) nuclear excitations, $K_{vib}(U')$ and $K_{rot}(U')$ - are coefficients of level density enhancement due to vibrational and rotational states at the effective excitation energy U'.

The energy dependence of the quasiparticle level density has been calculated on the basis of superfluid nuclear model [35]. The correlation function for the ground states of nuclei was defined as $D_0 = 12.0/A^{1/2}$ MeV. This choice of D_0 is consistent with the systematics of nuclear masses [36] and with the results of analysis of the experimental data on neutron resonances for heavy nuclei [35]. The

critical temperature of the phase transition from superfluid to normal state, the condensation energy, the critical energy of the phase transition and the effective excitation energy are connected with correlation function D_0 by the following equations:

$$t_{cr} = 0.567 D_0$$
$$U_{cr} = 0.472 a_{cr} D_0^2 - n D_0 \qquad (19)$$
$$E_{con} = 0.152 a_{cr} D_0^2 - n D_0$$
$$U' = U + n D_0 + \delta_{shift} ,$$

where $n = 0,1$ and 2 for even-even, odd and odd-odd nuclei, correspondingly, and the empirical value of the excitation energy shift δ_{shift} chosen on the base of consistent description of the level density of low lying collective levels and data on neutron resonances.

The shell effects were included into consideration using the energy dependence of nuclear level density parameter $a(U,A)$ determined phenomenologically:

$$a(U,Z,A) = \tilde{a}(A) \cdot \left(1 + \delta W(Z,A) \cdot \frac{f(U'-E_{cond})}{U'-E_{cond}} \right), \quad U' > U_{cr}$$
$$a(U,Z,A) = a(U_{cr},Z,A), \quad U' < U_{cr} , \qquad (20)$$

where the asymptotic value of level density parameter at high excitation energy is equal to

$$\tilde{a}(A) = 0.073A + 0.115A^{2/3} , \qquad (21)$$

where $\delta W(Z,A)$ is the shell correction to nuclear binding energy defined from the experimental values of nuclear masses or in the case of their lack with the help of the Mayers-Swiatecki formula [37], $f(U)=\{1-\exp(-\gamma U)\}$ is the dimensionless function which defines the energy dependence of the level density parameter at low excitation energies, value $\gamma = 0.4/A^{1/3}$ was chosen from the description of density of neutron resonances.

The vibrational enhancement of nuclear level density was presented in the following form

$$K_{vib} = \exp\{ \delta S - (\delta U/t)\} , \qquad (22)$$

where δS, δU are the changes of entropy and excitation energy due to collective modes and defined from relations for Bose-particle gas

$$\delta S = \sum_{i=1}^{\infty} (2 l_i + 1)\left\{(1+n_i)\ln(1+n_i) - n_i \ln(n_i)\right\}$$
$$\delta U = \sum_{i=1}^{\infty} (2 l_i + 1) w_i n_i , \qquad (23)$$

where w_i and l_i are the energy and the multipolarity of collective excited state, n_i is its population for the corresponding temperature. The attenuation of vibrational enhancement of level density at high temperatures is taken into account with the following occupation number dependence:

$$n_i = \frac{\exp\{-g_i/(2w_i)\}}{\exp\{w_i/t\}-1}, \qquad (24)$$

through the parameter γ_i obtained empirically on consistent description of the low-lying levels and the data on neutron resonances

$$g = 0.0075A^{1/3}(w_i^2 + 4p^2t^2) . \qquad (25)$$

The quadrupole and octupole states were considered in the calculations only. The position of the lowest state for the all nuclei, with exception of ^{208}Pb, was defined by phenomenological equations which reproduced the experimental data well enough for middle weight nuclei:

$$w_2 = 30A^{-1/3}; \qquad w_3 = 50A^{-1/3} . \qquad (26)$$

For nucleus ^{208}Pb the position of 2^+ state was assumed to be equal to experimental value *4.1* MeV.

For all spherical nuclei the coefficient of vibrational enhacement of the level $K_{vibr}(U')$ was taken into account according equation (22) only. For deformed nuclei the enhancement of level density connected with rotational mode of collective excitation $K_{rot}(U')$ was taken into account according to Ref. [35] :

$$K_{rot}(U) = s_{\wedge}^2 \cdot g(U) = s^2 \cdot (1 + b/3) \times g(U) , \qquad (27)$$

where s is the spin cut-off factor, and $g(U)$ is the empirical function taking into account the attenuation of rotation modes at high energies proposed in Ref. [38]:

$$g(U) = \{1 + \exp[(U - U_r)/d_r]\}^{-1} , \qquad (28)$$

where the parameters of attenuation function are connected with the parameter of quadrupole nuclear deformation b by relations:

$$U_r = 120A^{-1/3}b^2 ; d_r = 1400A^{-2/3}b^2 . \qquad (29)$$

The parameter of quadrupole deformation was defined from formulae for nuclear masses [36].

The advantage of considered approach to obtain nuclear level density consists in calculation of cross-sections for magic and neighboring nuclei taking into account shell effects. As an example Figures 15,16 present the cross-sections for *(p,2n2p), (p,3n2p), (p,4n2p),* and *(p,6n4p)* reactions on ^{90}Zr calculated with the superfluid model and Fermi gas model of level density where $a = A/9.0$ was used. As seen from the Figures, the better agreement with experimental data in the whole energy range *0 - 100* MeV is observed in the case of level density calculation based on the superfluid model.

5. Equilibrium γ-ray emission

The probability of photon emission has been calculated through the following formula:

$$\Gamma_g(E) = \frac{1}{p^2 c^2 r(E)} \cdot \int e_g^2 s_g(E - e_g) r(E - e_g) de_g, \quad (30)$$

where s_g is the photon absorption cross-section. It has been obtained using the Lorenz formula:

$$s_g(e_g) = \sum_{k=1}^{2} \frac{s_k e_g^2 G_{kg}^2}{(e_g^2 - E_{kg}^2)^2 + e_g^2 G_{kg}^2}, \quad (31)$$

taking into account the splitting of dipole giant resonance in deformed nuclei. The position of maximum of dipole giant resonance was calculated taking into account the quadrupole deformation b in the following way [39]

$$E_{1g} = E_0 (1 - b/3)^2 ; E_{2g} = E_0 (1 - 0.16b); E_0 = 43.4A^{-0.215} . \quad (32)$$

The widths of the resonances are equal to:

$$G_i = 0.232E_1 ; G_2 = 0.232E_2 , \quad (33)$$

and the maximum values of photon absorption cross-sections are equal to

$$s_{1g} = 145.0 \times A/E_1 ; s_{2g} = 235.0 \times A/E_2 . \quad (34)$$

The nuclear level density for g-channel has been calculated on the basis of the superfluid model consistently with other reaction channels.

The importance of taking into account g-ray emission for some reactions induced by medium energy protons on neutron deficient nucleus in particular ^{124}Xe has been noted [40]. The taking into account the competition of g-rays and particle emission permits to avoid sharp spurious peak near threshold region and to get a reasonable description of experimental data [40-44]. The calculations with ALICE-IPPE code using consistent level density parameters in gamma and particle channels can be considered as a reasonable cross-section evaluation for energy region up to *100* MeV.

References

1. A.J.Koning, Requirements for an Evaluated Nuclear Data File for Accelerator-Based Transmutation. NEA/NSC/DOC(93)6. NEA/P&T Report N^{o} 6.

   Yu.N.Shubin et al., MENDL Activation Data Library for Intermediate Energies. Report IAEA-NDS-136, Rev. 0, May 1994, Vienna 1994.

   F.M.Mann, Transmutation of Alloys in the MFE Facilities as Calculated by REAC (A Computer System for Activation and Transmutation). /HEDL-TME,81-37, (1982).
2. Yu.N.Shubin, V.P.Lunev, A.Yu.Konobeyev and A.I.Dityuk, Cross-Section Data Library MENDL-2 to Study Activation and Transmutation of Materials Irradiated by Nucleons of Intermediate Energies. *Report IAEA, INDC(CCP)-385,* Vienna 1995.
3. A.I.Dityuk, A.Yu.Konobeyev, V.P.Lunev, Yu.N.Shubin, Creation of neutron threshold reaction systematics. *Voprosy atomnoy nauki I tekhniki, Series Yadernye Constanty, M*., (1996), N^{o} 1.
4. A.Yu.Konobeyev, V.P.Lunev, Yu.N.Shubin, Pre-equilibrium emission of clusters. *Preprint-IPPE-2465*, Obninsk 1995.
5. M.Blann, Importance of the Nuclear Density Distribution on Pre-Equilibrium Decay. *Phys. Rev. Lett,* **28** (1972) p.757.
6. M.Blann, H.K.Vonach, Global Test of Modified Precompound Decay Models. *Phys. Rev.* **C28** (1983) p.1475.
7. K.Kikuchi, M.Kawai, *Nuclear Matter and Nuclear Interactions*, North-Holland, Amsterdam, 1968.
8. A.Iwamoto, K.Harada, Mechanism of Cluster Emission in Nucleon-Induced Preequilibrium Reactions. *Phys. Rev.* **C26** (1982) p.1821.
9. N.Sato, A.Iwamoto, K.Harada, Preequilibrium Emission of Light Composit Particles in the Framework of the Exciton Model. *Phys. Rev.* **C28** (1983) p.1527.
10. E.Gadioli, Emission of complex particles in precompound reactions., Report of Instituto Nazionale di Fisica Nucleare., (1988) Milano, Italy, INFN/BE-88-2.
11. E.Dobes, E.Betak, Proc. Int. Conf. React. Models 77, Balatonfured, (1977), p.195.
12. C.Kalbach, The Griffin Model, Comlex particles and Direct Nuclear Reactions., *Z.Physik,* **A283** (1977), p.401
13. E.Gadioli, E.Gadioli Erba, L.Glowacka, M.Jaskola, J.Turkiewicz, L.Zemlo, J.Dalmas and A.Chiadli, ^{90,91}Zr(n,α)^{87,88}Sr Reactions at 14.3 and 18.15 MeV Incident Neutron Energy. *Phys.Rev.* **C34** (1986) p.2065.

14. L.Milazzo-Colli and G.M.Braga-Marcazzan, α-Emission by Pre-equilibrium Processes in (n,α) Reactions. *Nucl.Phys.* **A210** (1973) p.297.

15. A.Ferrero, E.Gadioli, E.Gadioli Erba, I.Iori, N.Molho and L.Zetta, α-Emission in Proton Induced Reaction. *Z.Phys.* **A293** (1979) p.123.

16. Z.Lewandowski, E.Loeffler, R.Wagner, H.H.Mueller, W.Reichart, P.Schober, E.Gadioli and E.Gadioli Erba, Proton Induced α- and τ- Emission at 72 MeV. *Lett.Nuovo Cim.* **28** (1980) p.15.

17. E.Gadioli, E.Gadioli Erba, W.Augustyniak, L.Glowacka, M.Jaskola, J.Turkiewicz, and J.Dalmas, Alpha-particle emission from fast-neutron-induced reactions on neodymium isotopes. *Phys.Rev.* **C38** (1988) p.1649.

18. E.Gadioli, S.Mattioli, W.Augustyniak, L.Glowacka, M.Jaskola, J.Turkiewicz, and A.Chiadli, Structure Effects in the Spectra of α Particles from the Interaction of 12 to 20 MeV Neutrons with Samarium Isotopes. *Phys.Rev.* **C43** (1991) p.1932.

19. J.R.Wu, C.C.Chang and H.D.Holmgren, Charged Particle Spectra: 90 MeV Protons on ^{27}Al, ^{58}Ni, ^{90}Zr and ^{209}Bi. *Phys.Rev.* **C19** (1979) p.698.

20. A.Iwamoto and K.Harada, Mechanism of cluster emission in nucleon-induced preequilibrium reactions. *Phys.Rev.* **C26** (1982) p.1821.

21. A.Yu.Konobeyev and Yu.A.Korovin, Calculation of Precompound α-particle Spectra for Nucleon Induced Reactions on the Bases of Hybrid Exciton Model. *Kerntechnik,* **59** (1994) p.72.

22. P.Oblozinsky and I.Ribansky, Emission Rate of Preformed α-Particles in Preequilibrium Decay. *Phys.Lett,* **B74** (1978) p.6.

23. E.Gadioli and E.Gadioli Erba, Interpretation of the Continuous Spectrum of Secondary α Particles. *Z.Phys.* **A299** (1981) p.1.

24. S.G.Kadmensky and V.I.Furman, *Alpha-decay and nuclear reactions,* Moscow, Energoatomizdat, 1985.

25. I.Kumabe, Y.Inenaga, M.Hyakutake, N.Koori, Y.Watanabe, K.Ogawa and K.Orito, Alpha-particle Energy Spectra from the (p,α) Reaction on Nuclei around Atomic Number 50. *Phys.Rev.* **C38** (1988) p.2531.

26. A.Ferrero, I.Iori, N.Molho and L.Zetta, (p,α) Reactions on ^{93}Nb, ^{107}Ag, ^{118}Sn, ^{165}Ho, ^{169}Tm from 20 to 44 MeV Incident Proton Energy. *Report Instituto Nazionale di Fisica Nucleare, INFN/BE-78/6, December 1978,* Milano.(1978)

27. F.E.Bertrand and R.W.Peelle, Complete Hydrogen and Helium Particle Spectra from 30- to 60 MeV Proton Bombardment of Nuclei with A=12 to 209 and Comparison with the Intranuclear Cascade Model. *Phys.Rev.* **C8** (1973) p.1045.

28. A.Chevarier, N.Chevarier, A.Demeyer, G.Hollinger, P.Pertosa and Tran Minh Duc, Pre-equilibrium Alpha Emission Induced by Different Incident Channels: Evidence for Alpha Preformation in Nuclei. *Phys.Rev.* **C11** (1975) p.886.

29. A.Yu.Konobeyev, V.P.Lunev and Yu.N.Shubin, Semi-Empirical Systematics for (n, α) Reaction Cross Sections at the Energy of 14.5 MeV. *Nucl.Instr.Meth*, ser.**B108** (1996) p.233.

30. O.T.Grudzevich, A.V.Zelenetsky and A.B.Pashchenko, The KOP Code for the Calculations of Cross-Sections for the Interactions of Neutrons and Charged Particles with Atomic Nuclei based on the Optical Model. *Report of Institute of Physics and Power Engineering*, **N1802** (1986), Obninsk, USSR.

31. J.R.Huizenga and G.Igo, Theoretical Reaction Cross Sections for Alpha Particles with an Optical Model. *Nucl.Phys.* **29** (1962) p.462.

32. S.M.Grimes, R.C.Haight, K.R.Alvar, H.H.Barschall and R.R.Borchers, Charged Particle Emission in Reactions of 15 MeV Neutrons with Isotopes of Chromium, Iron, Nickel and Copper. *Phys.Rev.* **C19** (1979) p.2127.

33. M.V.Kantelo and J.J.Hogan, Radiochemical Study of Alpha Particle Emission in Reactions of ^{202}Hg with 10-86 MeV Protons. *Phys.Rev.* **C13** (1976) p.1095.

34. A. V.Ignatyuk, Contribution of collective modes to level density of excited nuclei., *Yadernaya Fizika*, **21** (1975) p.20

    A.I.Blokhin, A.V.Ignatyuk, A.B.Pashchenko, Yu.V.Sokolov and Yu.N.Shubin, Analysis of threshold reaction excitation functions in frame of unified superfluid model. *Comm Acad.of Science of USSR* **49** (1985) p.962.

    A.I.Blokhin, A.V.Ignatyuk and Yu.N.Shubin, Vibrational enhancement of the level density of nuclei in the iron region. *Sov.J.Nucl.Phys.* **48(2)** (1988) p.232.

    A.V.Ignatyuk, J.L.Weil., S.Raman and S.Kahane, Density of Discrete Levels in ^{116}Sn. *Phys. Rev.* **C47** (1993) p.1504.

35. A.V.Ignatyuk, K.K.Istekov, G.N.Smirenkin, The role of collective effects for nuclear level density systematics. *Yad. Fiz.* **29** (1979) p.875.

36. W.D.Myers, Droplet Model of Atomic Nuclei, IFI/Plenum Press N.Y. 1977

37. W.D.Mayers and W.J.Swiatecki, Anomalies in Nuclear Masses. *Arkiv for Fysik* **36** (1967) p.343.

38. G.Hansen and A.S.Jensen, Energy dependence of the rotational enchancement factor in the level density. *Nucl.Phys.* **A406** (1983) p.236

39. M.Blann, G.Reffo, F.Fabbri, Calculation of γ-ray Cascades in Code ALICE. In: *Proc. Meeting on Methods for the Calculations of Neutron Nuclear Data.* Bologna, Italy, 1986, p.107

40. Yu.N.Shubin, Rep. in *IAEA Advisory Group Meeting on Intermediate Energy Nuclear Data for Applications.* Vienna (1990)

V.P.Lunev et al., An Analysis of Reaction cross section Calculation Methods for the Production of Medical Radioisotopes. In: *Proc. Int. Conference on Nuclear Data for Science and Technology*. Julich (1991) p.609.

M.Blann et al., Effect of Gamma Emission Competition on the Excitation Function Description for the Reactions Induced by Medium Energy Nucleons. In: *Proc. Int. Conference on Nuclear Data for Science and Technology*. Gatlinburg (1994) p. 539.

41. N.V.Kurenkov et al., Excitation functions of proton-induced nuclear reactions on ^{124}Xe: Production of ^{123}I. *J.Radioanal.Nucl.Chem.Lett.* **135** (1989) p.39.

42. F.T rk nyi et al., Excitation Function of (p,2n) and (p,pn) Reactions and Differential and Integral Yeilds of ^{123}I in Proton Induced Nuclear Reactions on Highly Enriched ^{124}Xe. *Appl. Rad.Isot*. **42**,(1991), p.221.

43. F.T rk nyi et al., Nuclear Reaction Cross Section Relevant to the Production of the ^{122}Xe-^{122}I Generator System using Highly Enriched ^{124}Xe and a Medium-sized Cyclotron. *Appl. Rad.Isot*. **42** (1991) p.229.

44. N.I.Venikov et al., Excitation functions of proton-induced reactions on ^{126}Xe: ^{125}I Impurity in ^{123}I. *Appl. Rad.Isot*. **44** (1993), p.51.

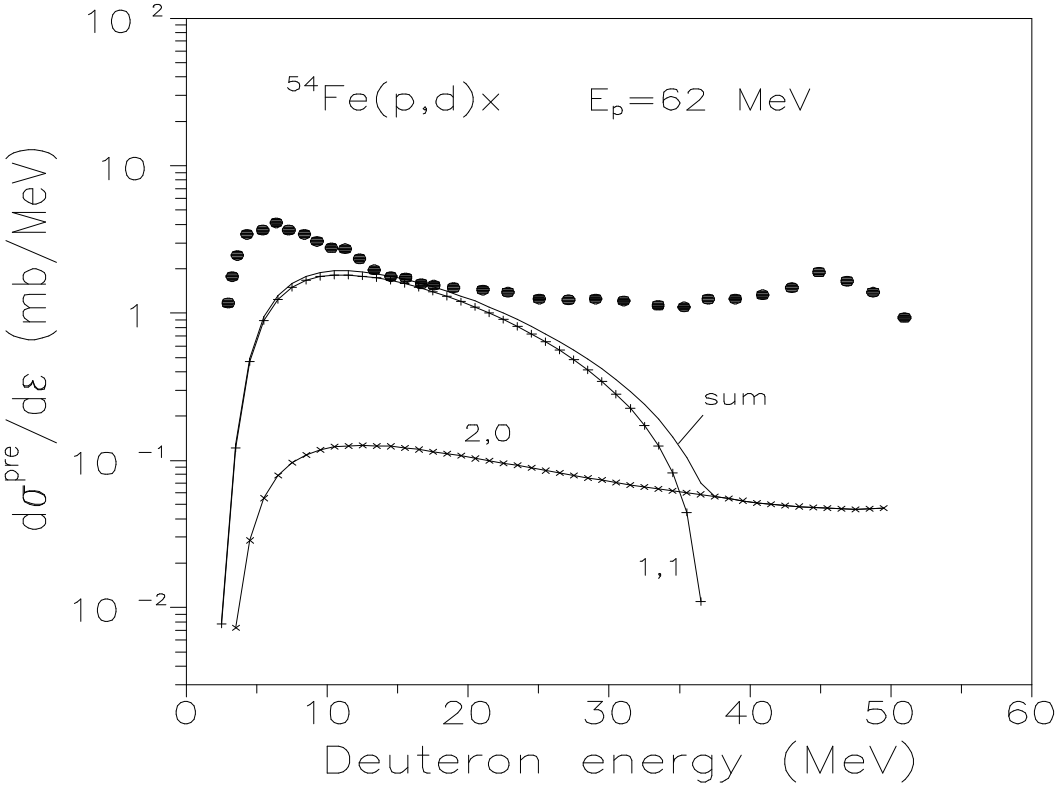

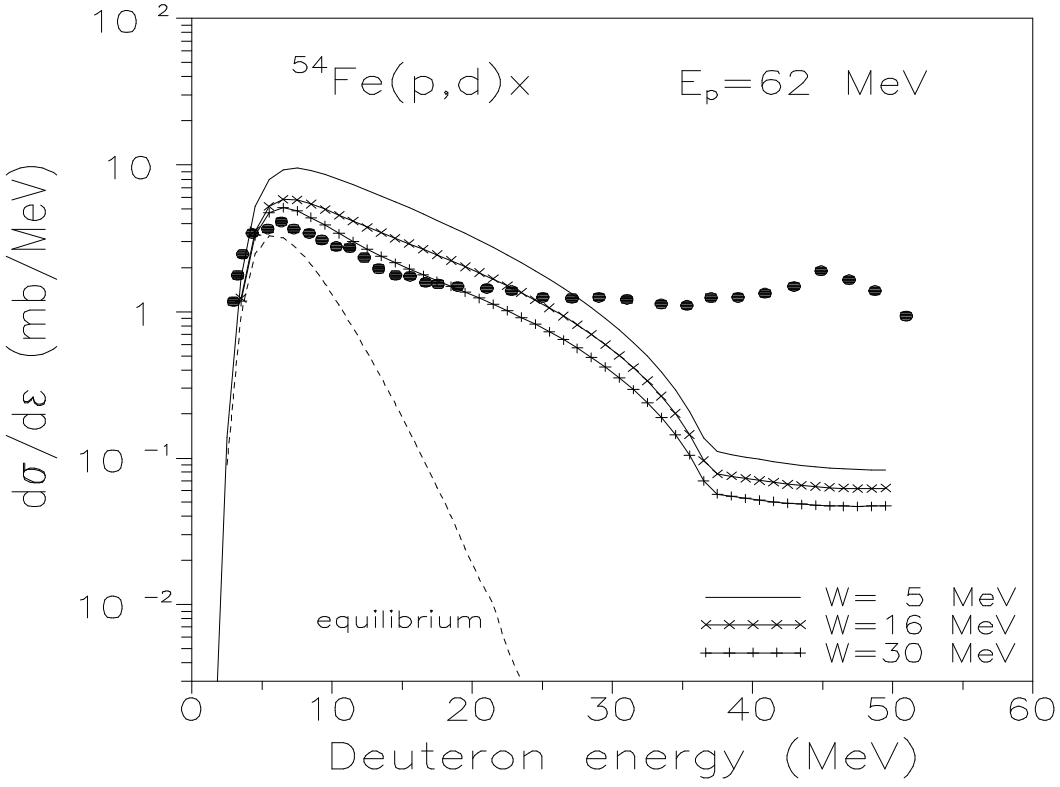

Fig.1. Deuteron emission spectra calculated without taking into account the direct processes. The upper Figure presents the precompound deuteron spectrum as well as the $F_{1,1}$ and $F_{2,0}$ [9] contribution components. The lower Figure shows the total deuteron spectrum obtained provided the precompound calculations have been perfomed using different values of the deuteron optical potential imaginary part *W*.

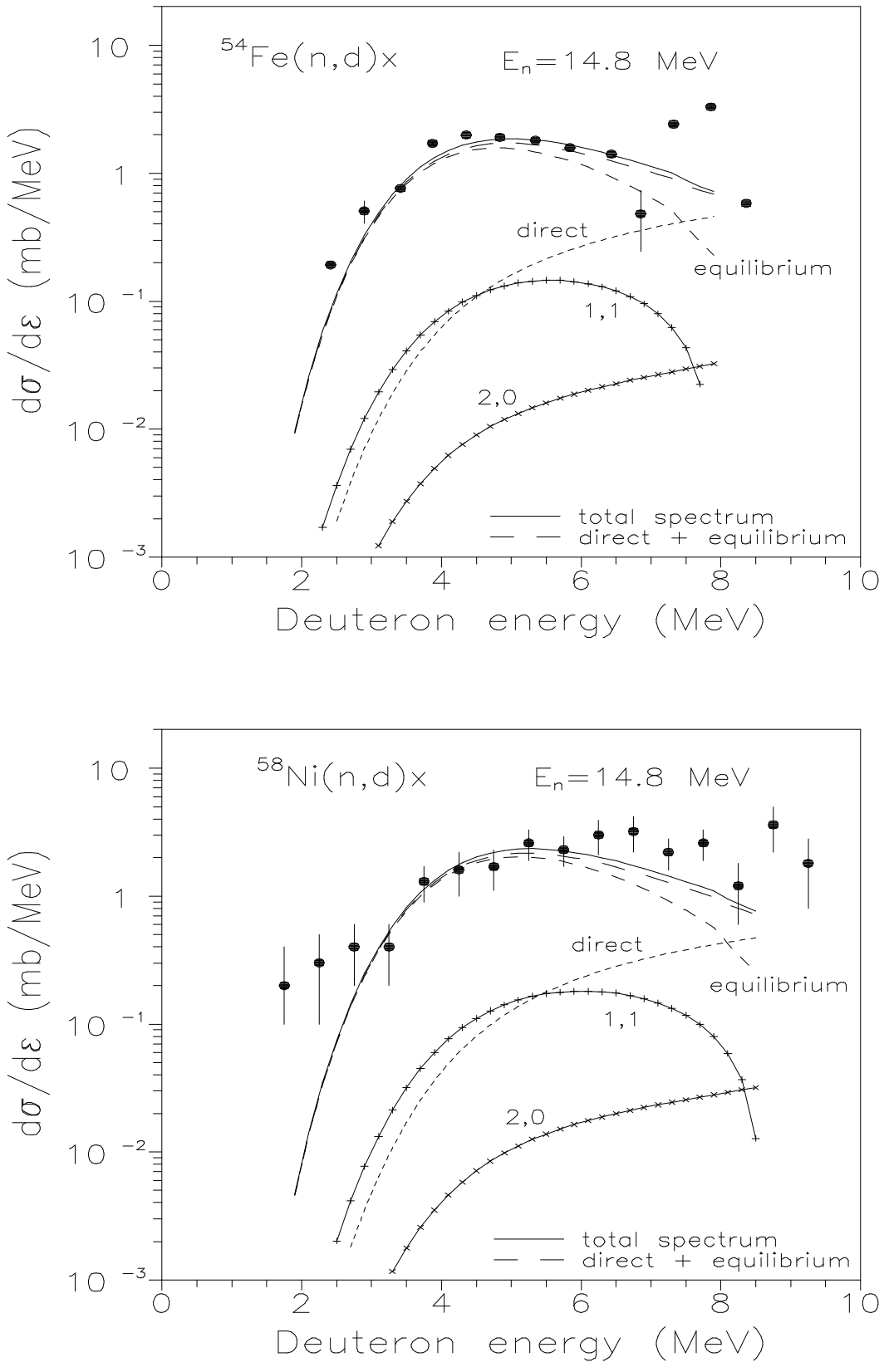

Fig.2. Calculated deuteron emission spectra for 14.8 MeV incident neutron induced reactions on ^{54}Fe and ^{58}Ni. The contributions of the direct processes, $F_{1,1}$ and $F_{2,0}$ precompound and equilibrium processes are shown.

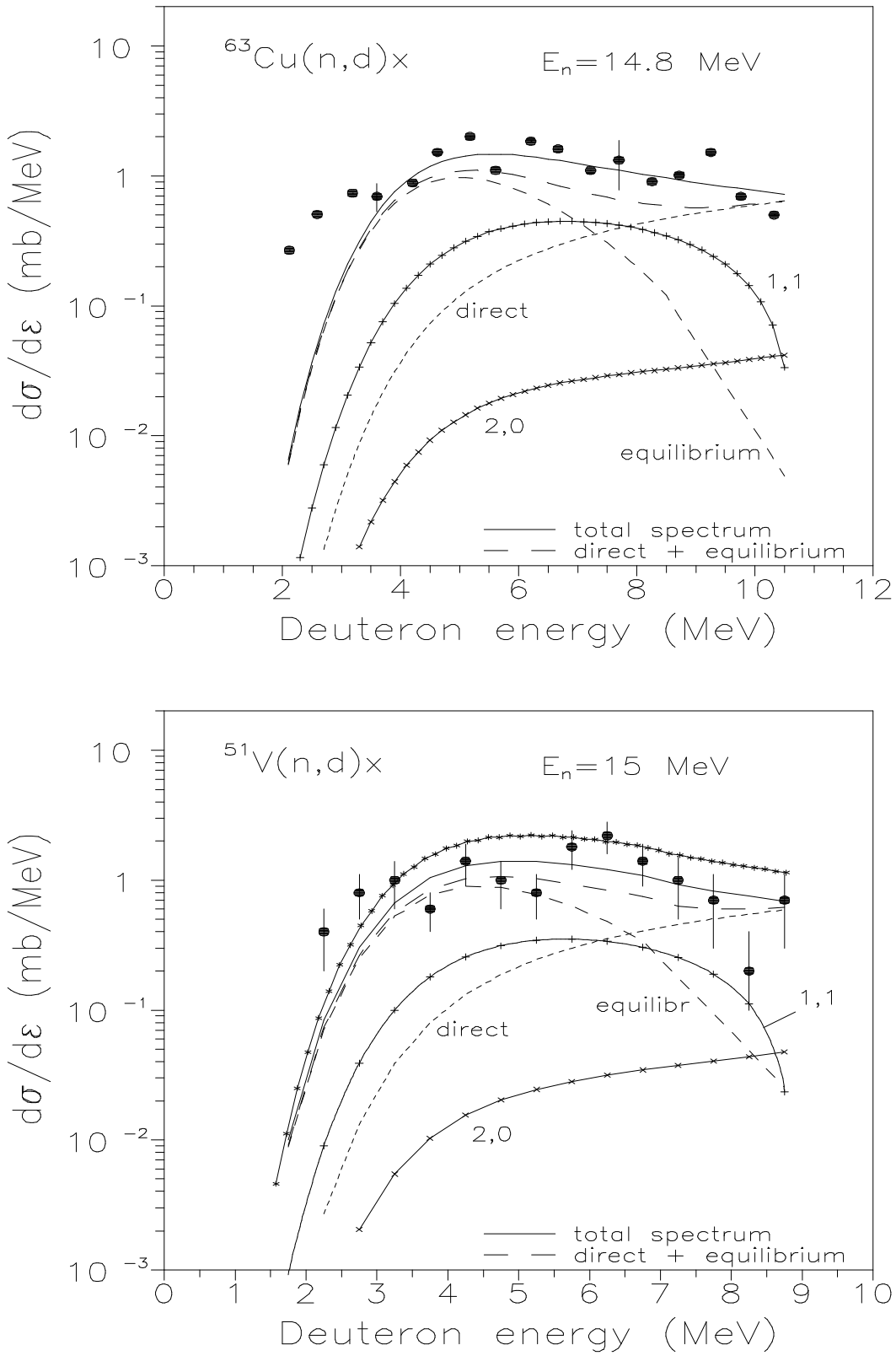

Fig.3. The same as in Fig.2, for ^{63}Cu and ^{51}V.

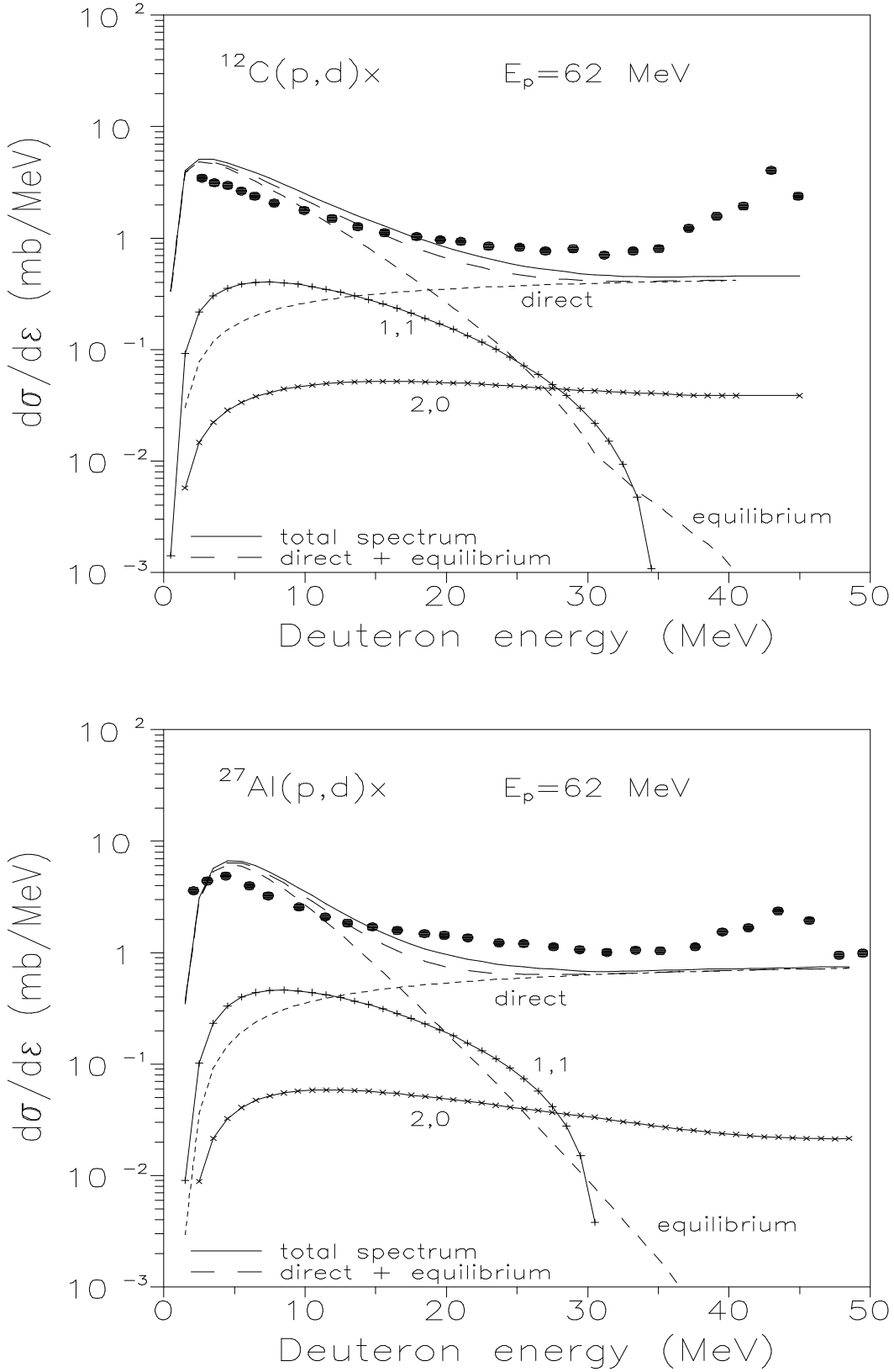

Fig.4. Deuteron spectra calculated at 62 MeV proton energy for ^{12}C and ^{27}Al.

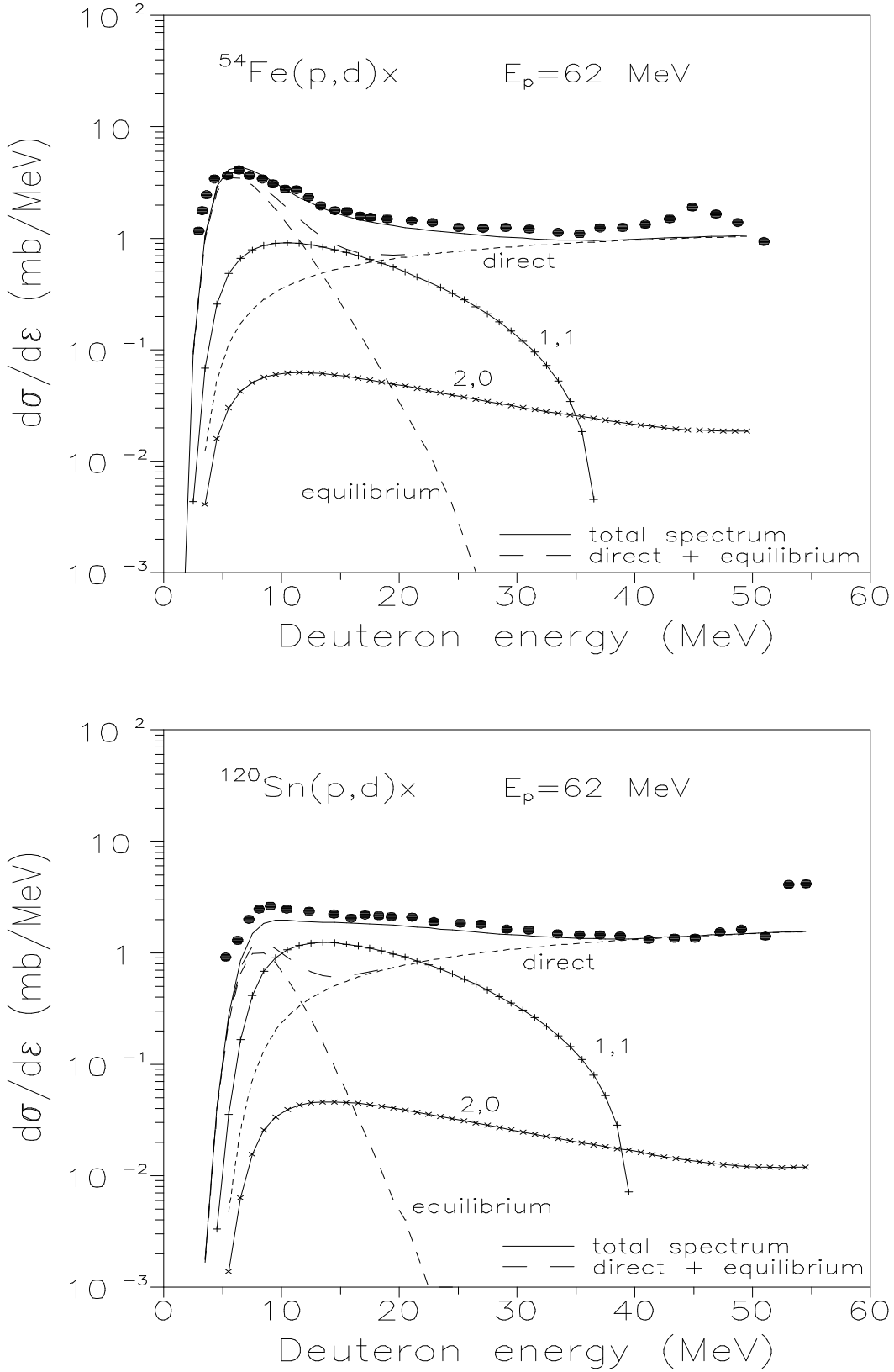

Fig.5. The same as in Fig.4, for ^{54}*Fe(p,d)* and ^{120}*Sn(p,d)* ractions.

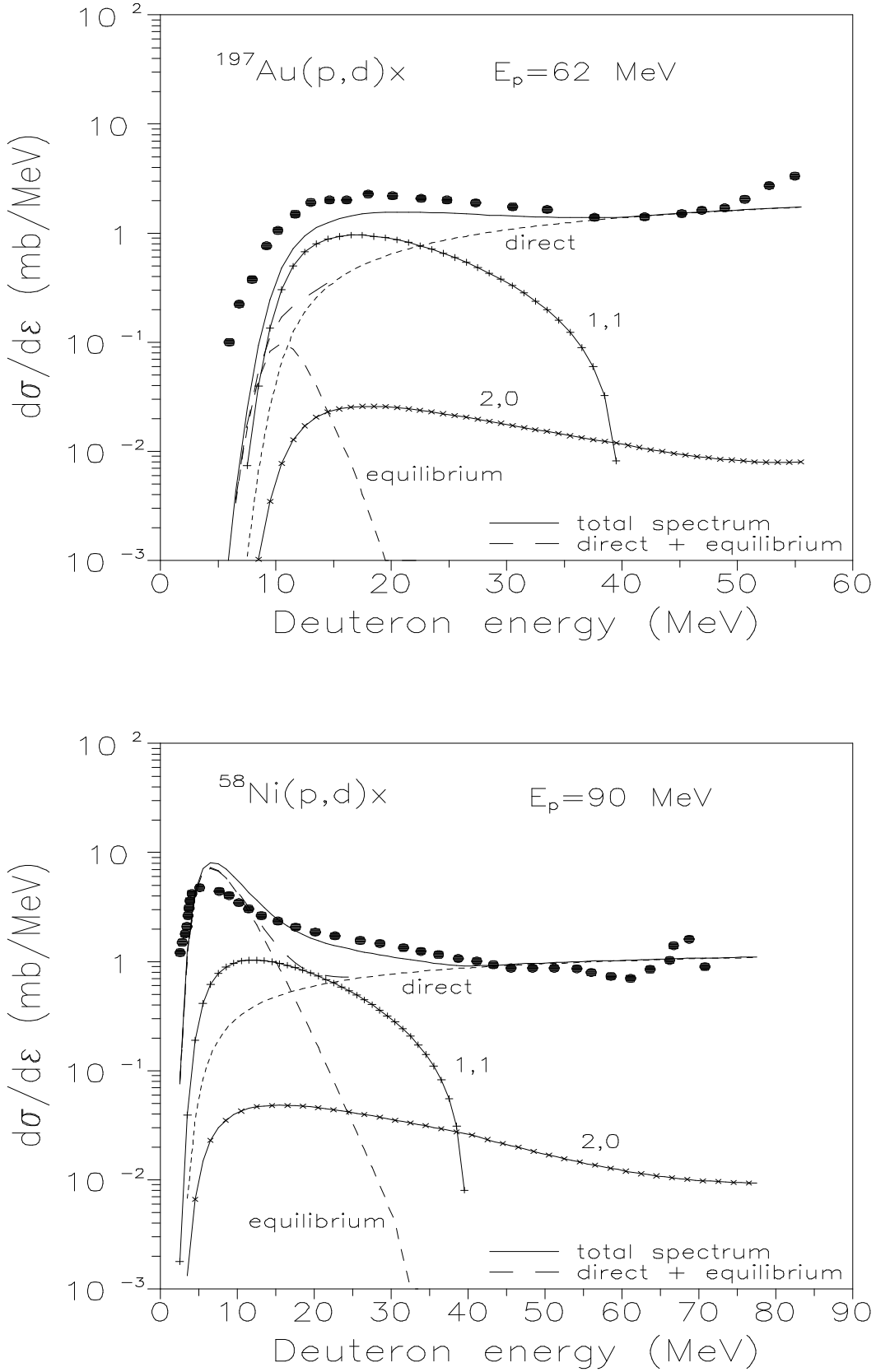

Fig.6. Calculated deuteron emission spectra for 90 MeV and 62 MeV proton induced reactions. The contributions of different processes to the emision spectra are shown.

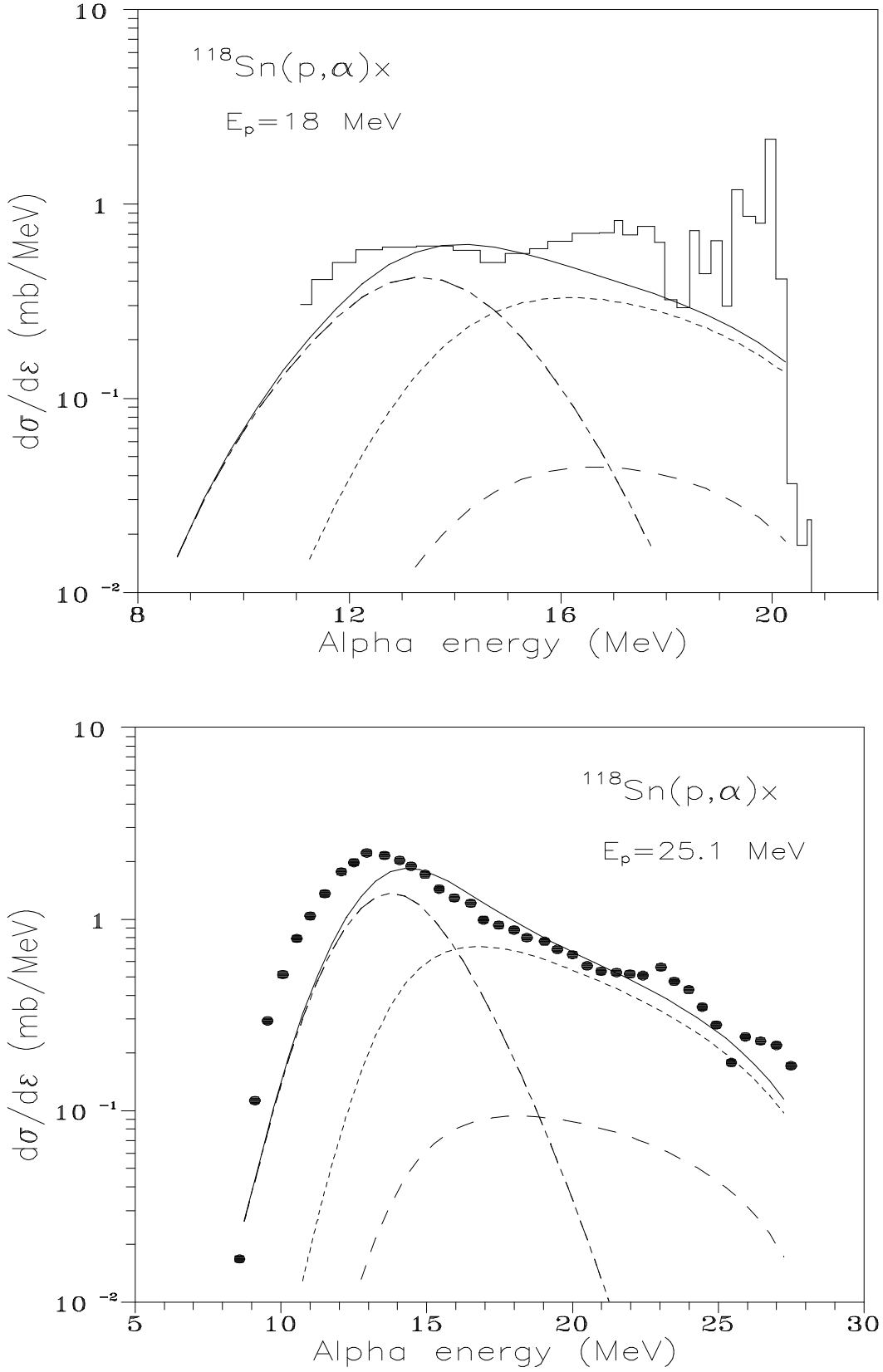

Fig.7. Experimental [25-27] (points) - α-spectra from the reactions on tin isotopes irridiated by 18-and 25.1 MeV protons. Total spectrum - (solid line), pick-up process contributions - (short dash line), knock-out - (long dash line), evaporation emission - (dash dot line).

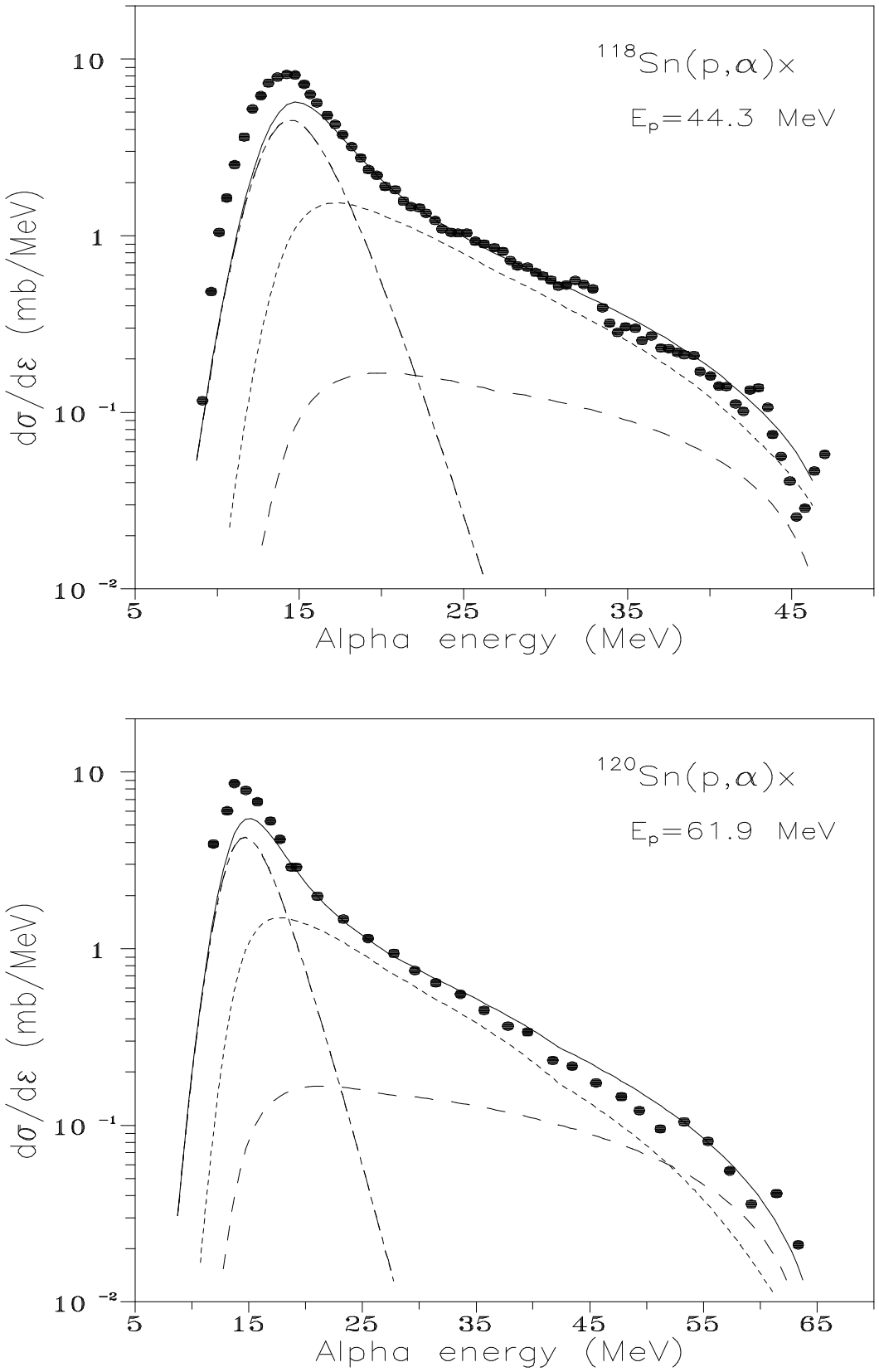

Fig.8. The same as in Fig.7, for 44.3 and 61.9 MeV.

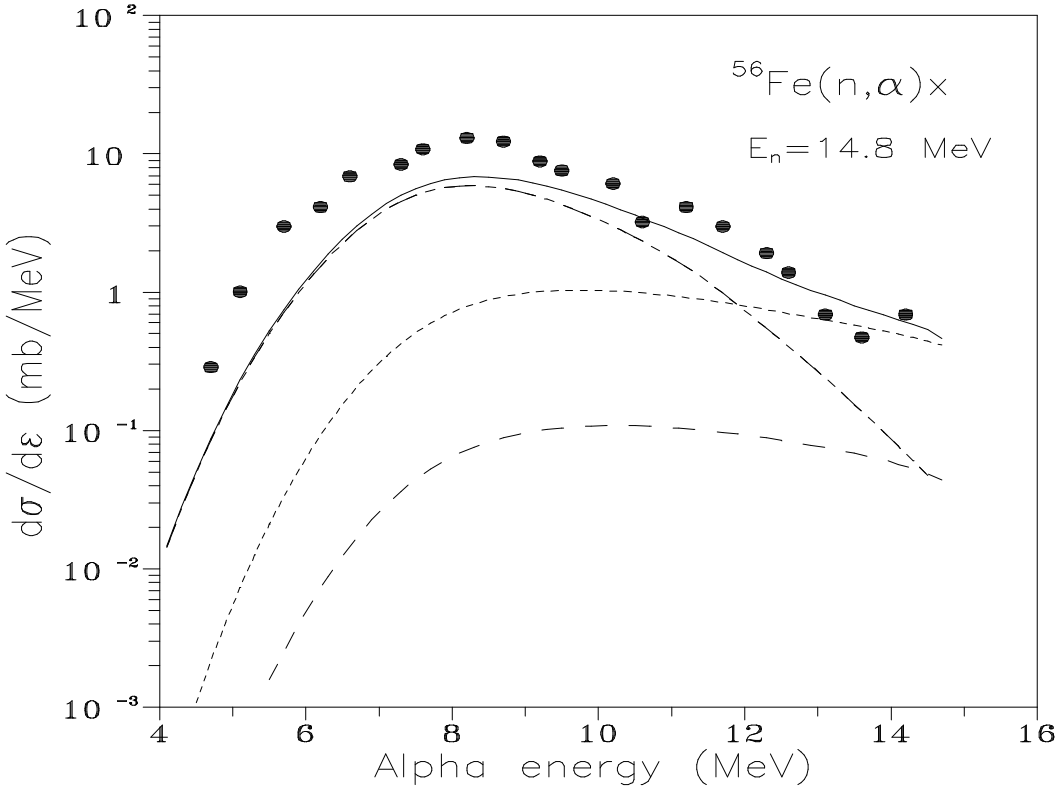

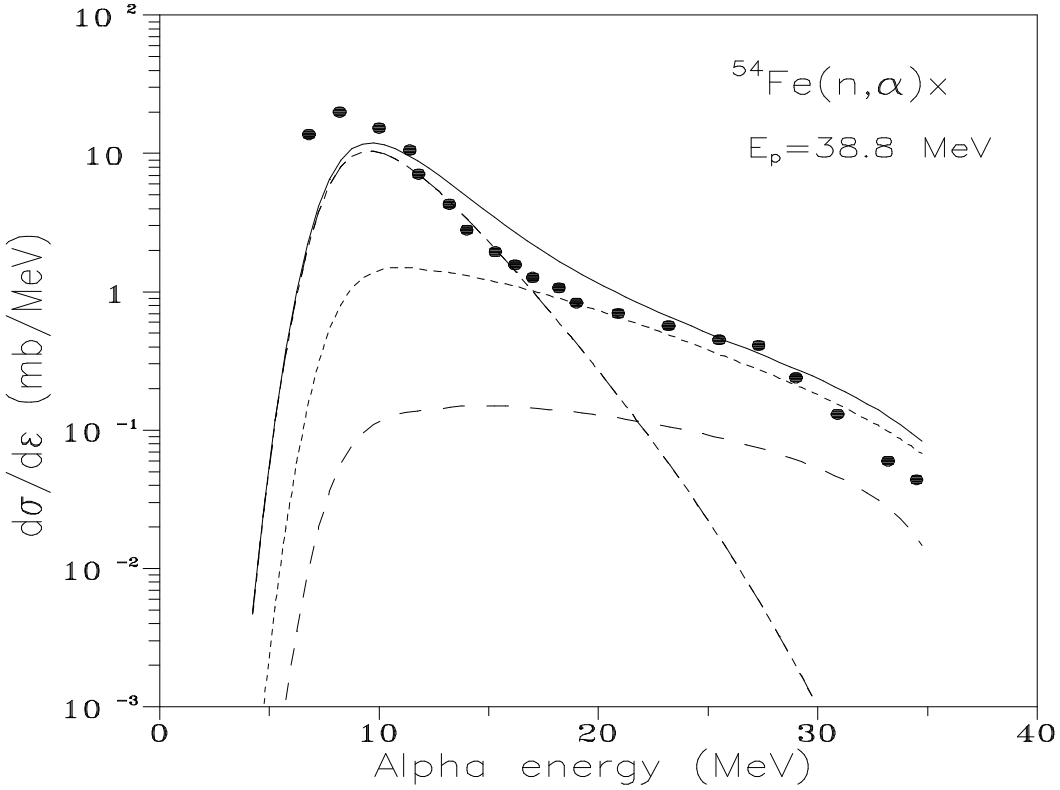

Fig.9. The same as in Fig.7 for the reactions on iron isotopes for various proton energies.

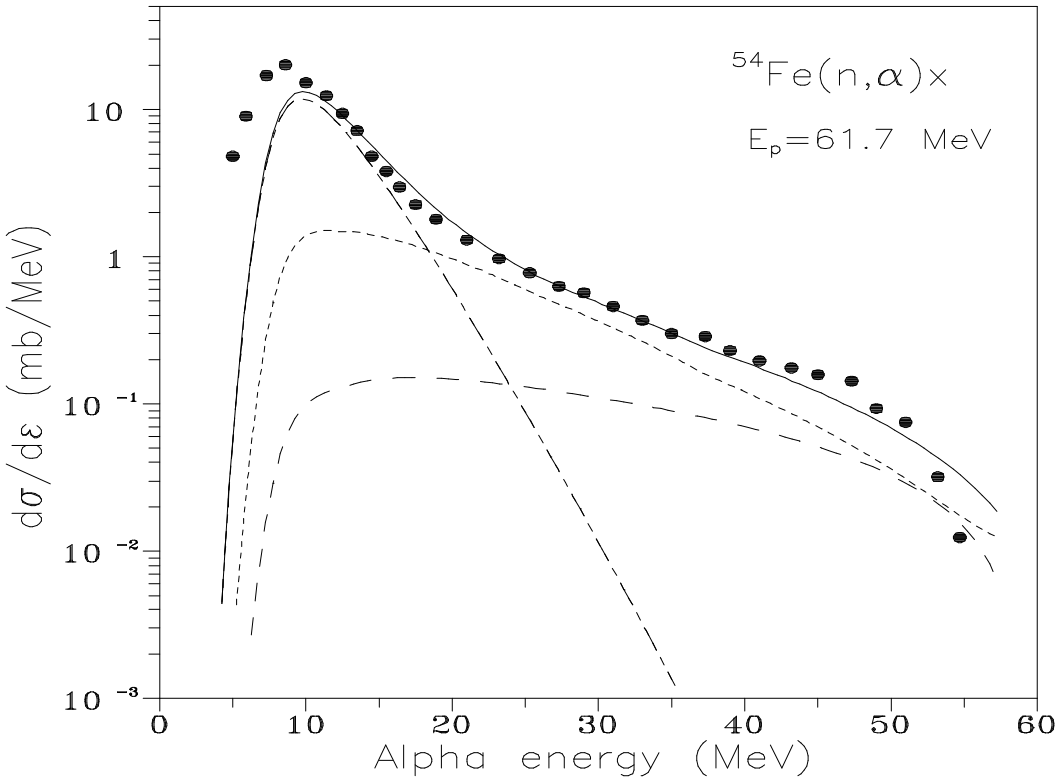

Fig.10. The same as in Fig.9. for the reaction on iron-54 at 61,7 MeV proton energy. Experimental data are taken from [27-32].

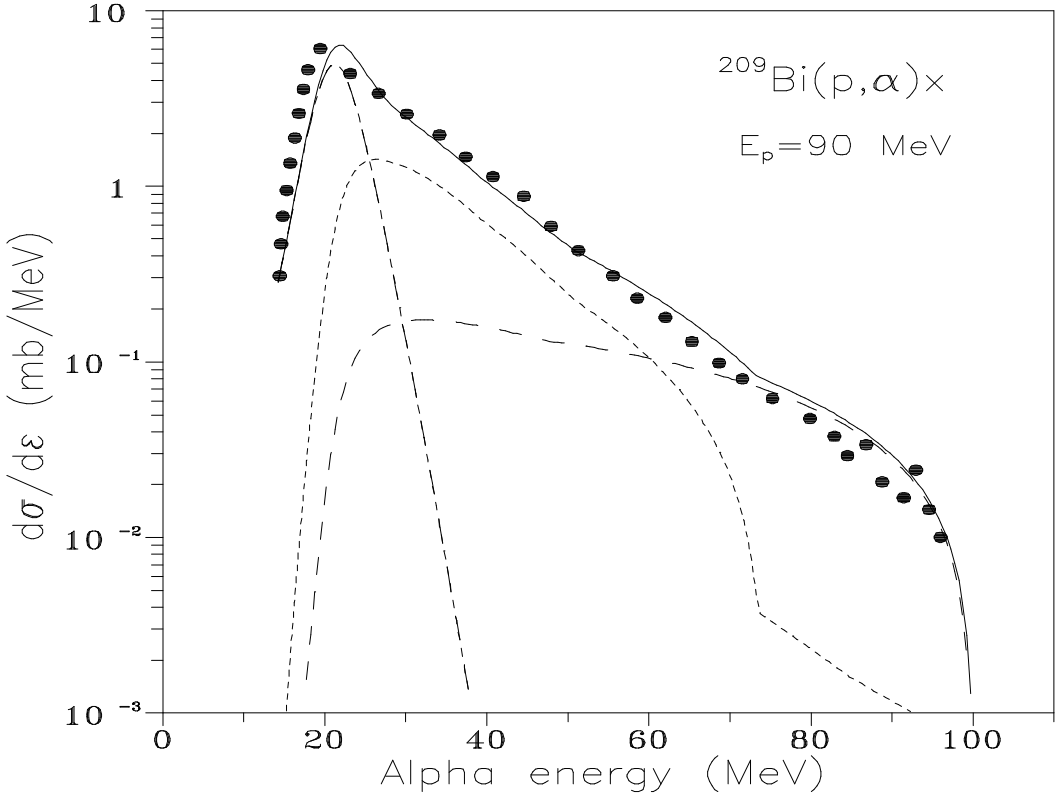

Fig.11. α-particle spectra from the reaction on ^{209}Bi irradiated with 90 MeV protons. Experimental data are taken from [19].

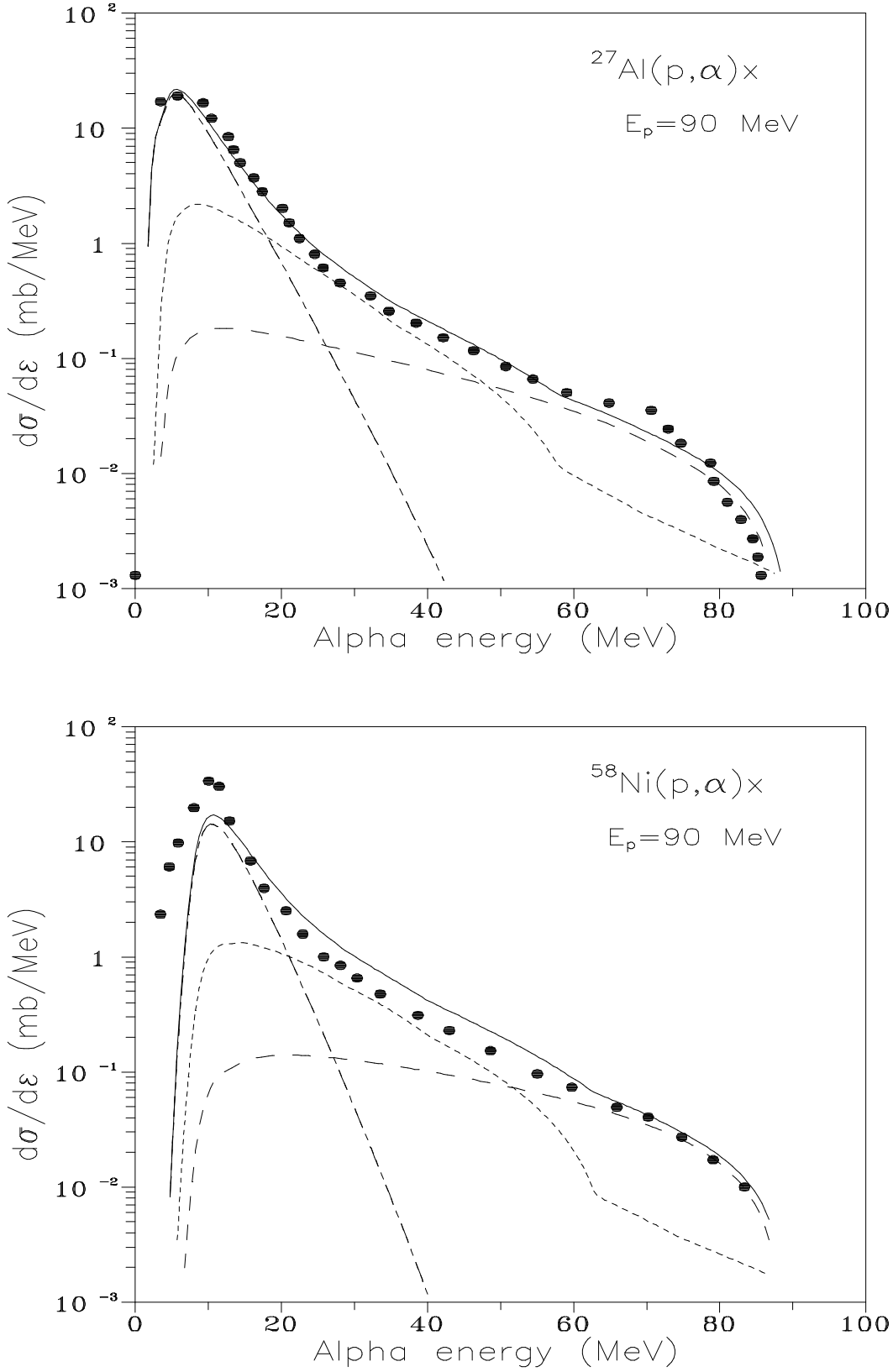

Fig.12. α-particle spectra from the reaction on ^{27}Al and ^{58}Ni irradiated with 90 MeV protons. Experimental data are taken from [19].

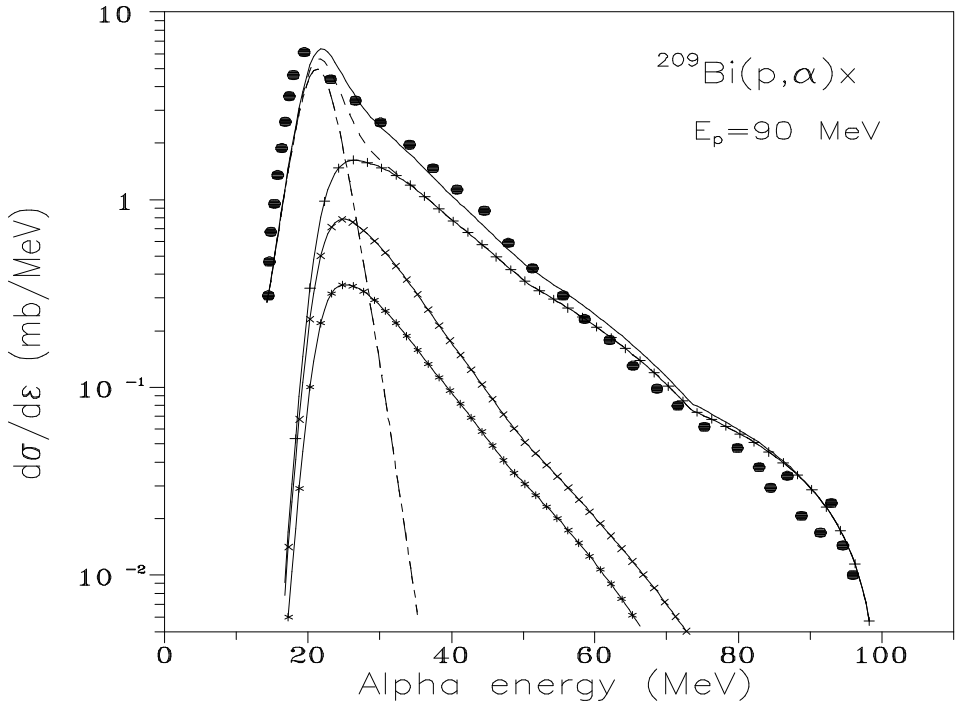

Fig.13. Calculated contributions of various α-emissions meshanisms to the total α-spectrum for the reactions on ^{209}Bi at 90 MeV proton energy. First preequilibrium α-particle - (+), preequilibrium α-particle emitted after neutron - (×) and proton - (*), equlibrium emission - (dash dot line), sum of the first preequilibrium a-particle and evaporation spectra - (dash line), total spectrum - (solid line).

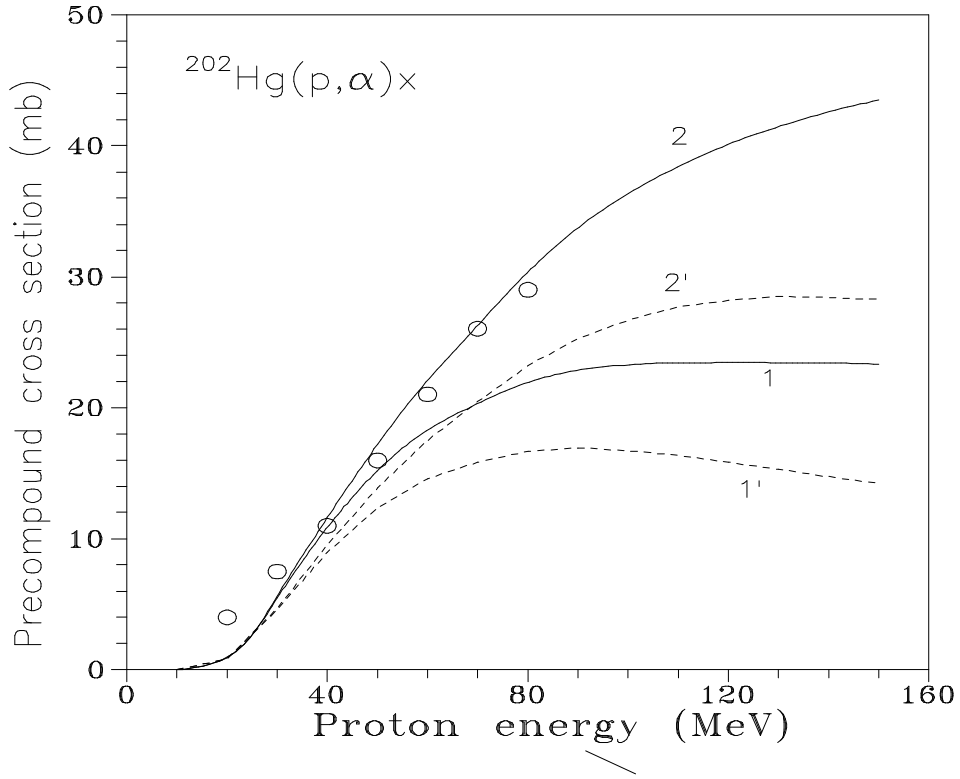

Fig.14. α-particle formation cross section at preequilibrium stage from reactions on ^{202}Hg irradiated by protons, calculated with - (2) and without - (1) taking into account multiple preequilibrium emission. Pick-up process contributions - dash lines (1') and (2'). Experimental data are taken from [34].

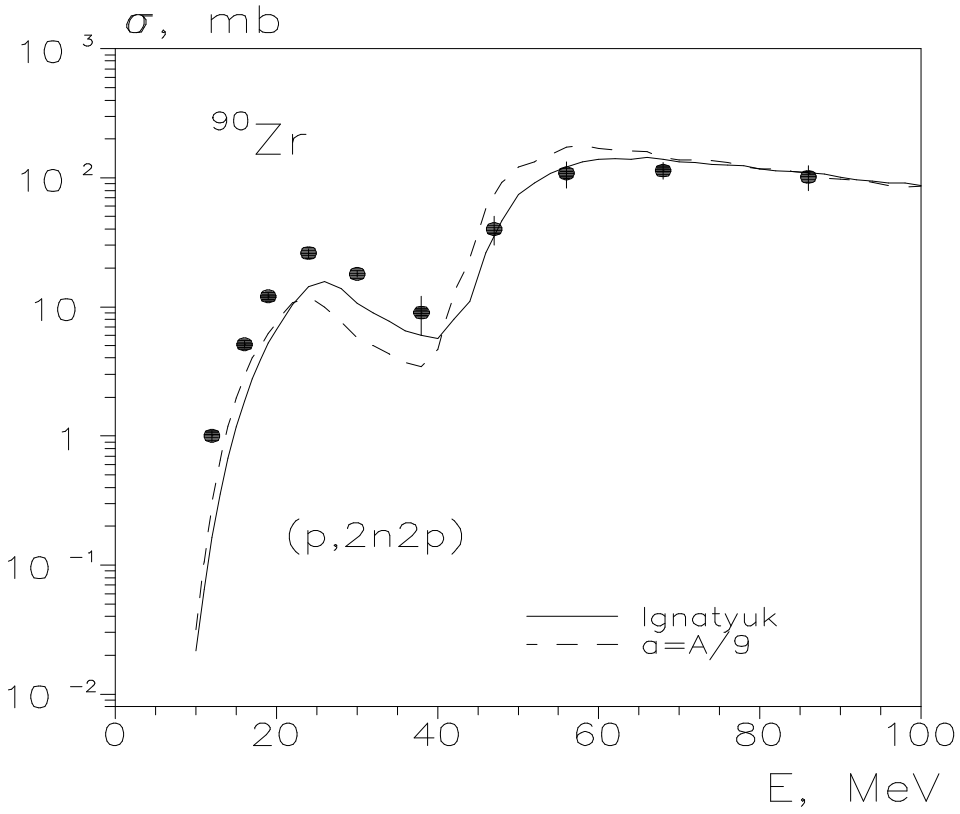

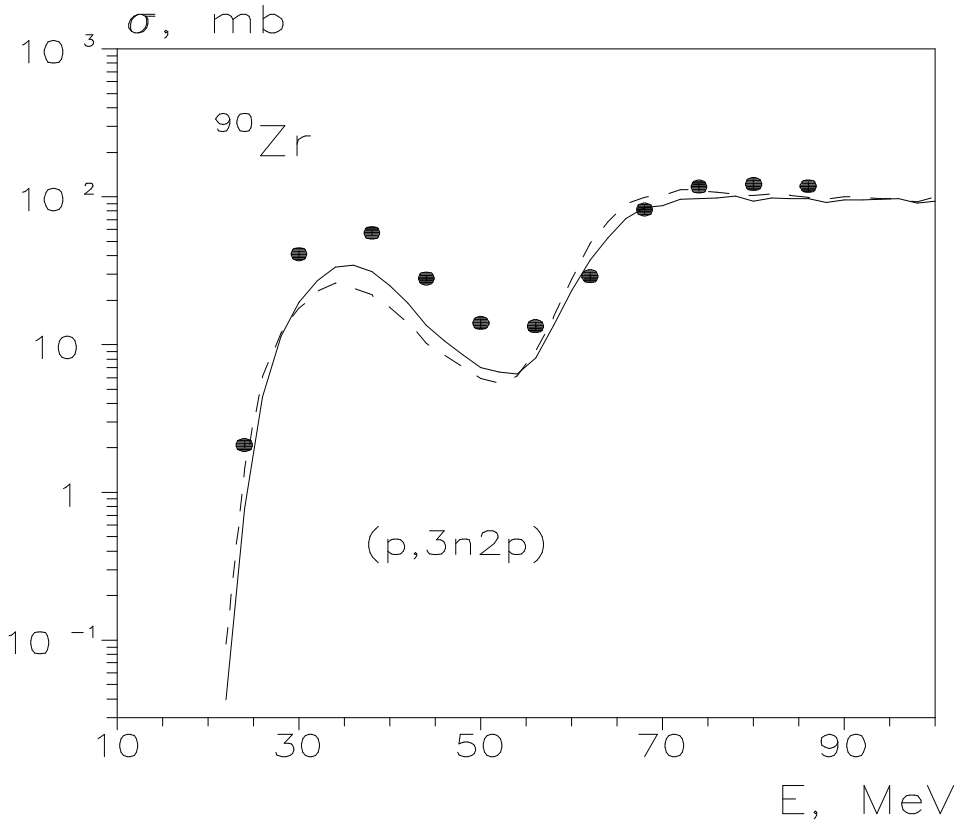

Fig.15. Effect of different models for level density calculations. Dashed line - calculations with Fermi-gas model *(a=A/9.0)* and solid line - superfluid model.

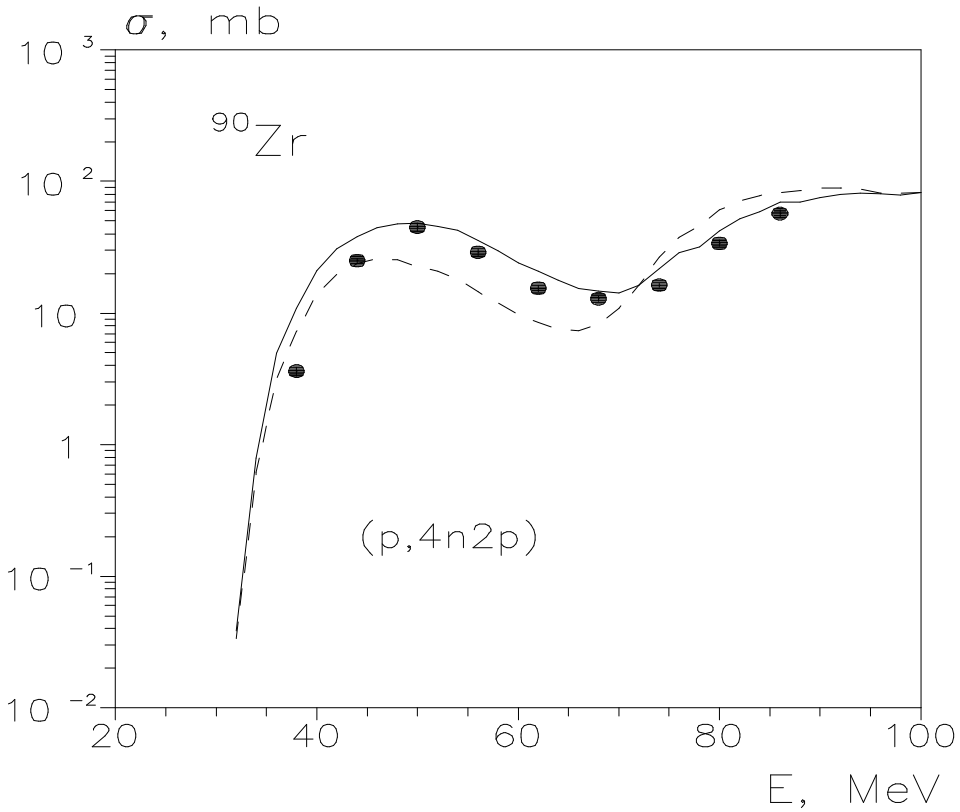

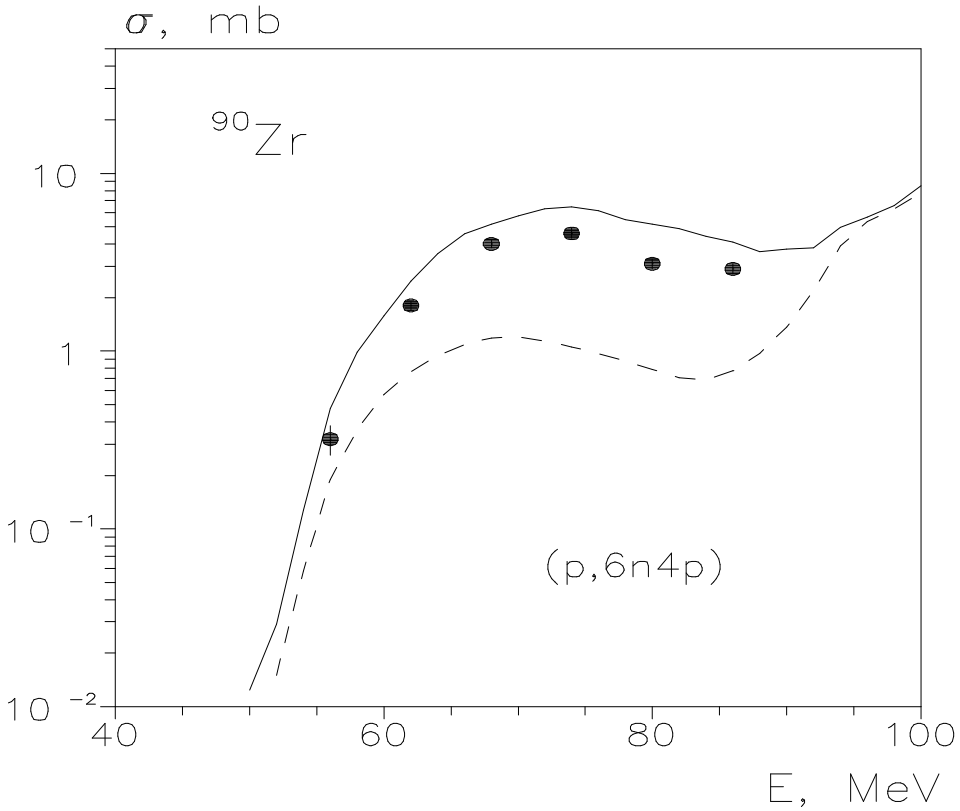

Fig.16. The same as in Fig.15.